Hindawi
Mathematical Problems in Engineering
Volume 2020, Article ID 4273810, 11 pages
https://doi.org/10.1155/2020/4273810

Research Article

Application of Similarity Theory for Dynamic Characteristics Prediction of Crane Flexible Truss Boom

Xuyang Cao, Zhiwei Wang, Wenjun Wang, and Xiang Dong

School of Mechanical Engineering, Dalian University of Technology, Dalian 116024, China

Correspondence should be addressed to Zhiwei Wang; duter_wzw@163.com

Received 5 January 2020; Accepted 20 February 2020; Published 19 March 2020

Academic Editor: Nhon Nguyen-Thanh

The aim of this study is to explore the similarity relations of dynamic characteristics of crane flexible truss boom. Combining perturbation theory with vibration analysis, a calculation method of the flexible boom natural frequency undergoing large overall rotary motion was proposed. According to the similarity theory, in terms of the geometrically similar truss boom, the similarity relations of their natural frequency and other parameters were derived. Taking the slenderness ratio of the actual product as the reference standard, two groups of scale-down crane truss boom experiments were designed. The results showed that, in aspect of the boom section size and the boom length, by using the similarity relations of the flexible boom, the dynamic characteristics can be predicted well.

1. Introduction

In order to meet the construction requirements of modern large-scale engineering projects, hoisting machinery is developing in the direction of towering and softening [1, 2]. However, the flexible deformation of the boom structure undergoing large overall motion is a difficult problem in boom design; relevant design specifications do not consider in depth the influence of the nonlinear dynamic characteristics of the boom on the operation accuracy and reliability [3] and thus lack effective theoretical guidance for serial design of boom. Similarity theory has the advantages of generality and rigorous digital derivation process, apply the similarity theory in the field of crane boom, derive similarity relations thus guiding boom design will become an efficiency design method.

Earlier engineering applications of similarity theory emerged in the analysis of fluid characteristic and geological experiments. Muller and Robertson [4] studied the similarity of specific shape objects motion in the wind field and water flow field. Silva [5] applied similarity theory to seismic tests under different environmental conditions. Since then, many scholars have done a great deal of researches in the field of marine structures, civil engineering structures, and power equipment through the principle of dynamic similarity [6–9]. Luo et al. [10] derived the similarity criterion of geomechanical magnetic model test according to the similarity relations between the magnetic field and the gravity field. Based on the similarity theory, Nam et al. [11] proposed a theoretical method of constructing a small gearbox with the same carrying capacity as a large one. Jha and Sedaghati [12] proposed the simulation quality to compensate the effect of gravity on the similarity relation in a similar model without considering the gravity. Wang et al. [13, 14] derived the complex shells dynamic similarity relations of underwater vibrations and the influence of the boundary effect on the similarity relation based on the equational analysis method and thus can be used to predict the vibration response of complex large-scale underwater structures accurately. Liu et al. [15] applied the moving boundary similarity method to underwater vibration and sound radiation research of the ship structure and analyzed the intrinsic relationship between underwater sound radiation and excitation frequency.

In the respect of crane operation and design, Dai et al. [16] applied the similarity theory to simulate the welding process of the swing arm of a large hydraulic excavator and derived the similarity rule of single-layer welding based on temperature field in certain conditions. Based on the dynamic similarity theory, Jin and Wu [17] derived the similarity scale

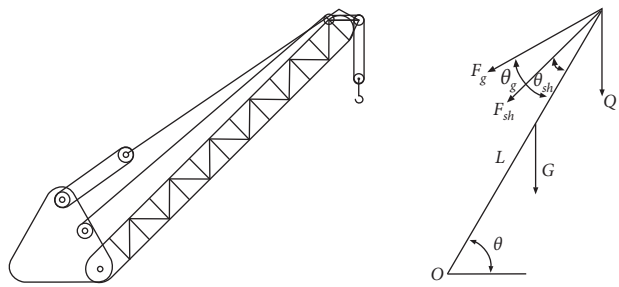

Figure 1: The force analysis in luffing plane.

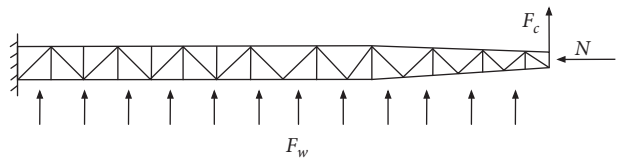

Figure 2: The force analysis in rotating plane. N is the axial force in luffing plane, F_w is the lateral load caused by inertial pendulum, and F_c is the lateral load caused by wind.

factor between the prototype structure and the scale-down model of quayside container crane analyzed and compared their respective dynamic characteristics and seismic responses. Chen and Sun [18, 19] established the dynamic model of overhead crane and proposed a novel control method by using the passivity property and the barrier Lyapunov function technique. Sun et al. [20] proposed a nonlinear motion control method of dual rotary crane system.

Aiming at the dynamic characteristics of the crane flexible boom, based on the flexible multibody dynamics theory, the truss boom of crawler crane is selected as the research object in this article, and the dynamic equation of the flexible truss boom is established. According to the numerical calculation results of the equation, the similarity relation of the dynamic parameters of the truss boom can be obtained based on the equational analysis method of similarity principle. The correctness of the similarity relation is verified by numerical calculation and similar model experiments.

2. Force Analysis of Crane Boom System

During crawler crane operation, boom actions can be divided into three different types, such as hoisting, luffing with payload, and rotating with payload; hoisting and luffing with payload occur in the luffing plane of the boom and rotating with payload occur in the swing plane of the boom.

As shown in Figure 1, when the force situation of the boom system is analyzed in the luffing plane, it can be simplified as an axially compressed simply supported beam whose base and top are hinged, where Q is the hoisting load, G is the weight of the boom structure, F_{sh} is the tensile force of the hoisting rope, F_g is the tensile force of the luffing plate, O is the hinge point of the boom and exterior structure, θ is the elevation angle of the boom, θ_{sh} is the angle between the hoisting rope and the boom axis, θ_g is the angle between the luffing rope and the boom axis, and L is the length of the boom.

When the force situation of the boom system is analyzed in the rotating plane, according to the restraint conditions, it can be simplified as a cantilever beam which is fixed at the base and unrestricted at the top, as shown in Figure 2. At the same time, the boom is subjected to axial force and lateral force in the rotating plane.

In this paper, the dynamic model of flexible boom will be established in the luffing plane and rotating plane.

3. Natural Frequency of Flexible Boom

3.1. Perturbation Theory for Natural Frequency of Flexible Boom. Whether in the luffing plane or the rotating plane, the flexible boom performs large overall rotary motion around the rotary center. For the structure of flexible boom, which has both large-scale movement and flexible deformation, the structure itself does not show the natural frequencies and vibration modes in traditional dynamical modal analysis [21]. Both the mass matrix and the stiffness matrix of the system are influenced by the angle of large overall rotary motion. From a time-varying perspective, system characteristic matrix is related to instantaneous angular velocity, which is a time-varying matrix. Therefore, in this paper, according to large overall rotary motion of the flexible boom, the perturbation method in mathematics is used to solve the approximate solution of its natural frequency.

When the flexible boom only does undamped free vibration in the equilibrium position without large overall motion, the dynamic equation is expressed as

$$M^{(0)}\ddot{q} + K^{(0)}q = 0, \tag{1}$$

where q is the state vector in the global coordinate system, $M^{(0)}$ is the free vibration mass matrix of the flexible boom, and $K^{(0)}$ is the free vibration stiffness matrix. The mass matrix and stiffness matrix are shown in Equations (2) and (3), respectively:

$$M^{(0)} = \begin{bmatrix} \frac{m}{3}c^2 + \frac{13m}{35}s^2 & \frac{m}{3}sc - \frac{13m}{35}sc & -\frac{11ml}{210}s & \frac{m}{6}c^2 + \frac{9m}{70}s^2 & \frac{m}{6}sc - \frac{9m}{70}sc & \frac{13ml}{420}s \\ & \frac{m}{3}s^2 + \frac{13m}{35}c^2 & \frac{11ml}{210}c & \frac{m}{6}sc - \frac{9m}{70}sc & \frac{m}{6}s^2 + \frac{9m}{70}c^2 & -\frac{13ml}{420}c \\ & & \frac{ml^2}{105} & -\frac{13ml}{420}s & \frac{13ml}{420}c & -\frac{ml^2}{140} \\ & & & \frac{m}{3}c^2 + \frac{13m}{35}s^2 & \frac{m}{3}sc - \frac{13m}{35}sc & \frac{11ml}{210}s \\ & & & & \frac{m}{3}s^2 + \frac{13m}{35}c^2 & -\frac{11ml}{210}c \\ sym & & & & & \frac{ml^2}{105} \end{bmatrix}, \tag{2}$$

$$K^e(q_i) = \begin{bmatrix} \frac{Ea}{l}c^2 & \frac{Ea}{l}cs & -\frac{6EI}{l^2}s & -\frac{Ea}{l}c^2 & -\frac{Ea}{l}cs & -\frac{6EI}{l^2}s \\ & \frac{Ea}{l}s^2 & \frac{6EI}{l^2}c & -\frac{Ea}{l}cs & -\frac{Ea}{l}s^2 & \frac{6EI}{l^2}c \\ & & \frac{4EI}{l} & \frac{6EI}{l^2}s & -\frac{6EI}{l^2}c & \frac{2EI}{l} \\ & & & \frac{Ea}{l}c^2 & \frac{Ea}{l}cs & \frac{6EI}{l^2}s \\ & & & & \frac{Ea}{l}s^2 & -\frac{6EI}{l^2}c \\ sym & & & & & \frac{4EI}{l} \end{bmatrix} + \begin{bmatrix} \frac{12EI}{l^3}s^2 & -\frac{12EI}{l^3}cs & 0 & -\frac{12EI}{l^3}s^2 & \frac{12EI}{l^3}cs & 0 \\ & \frac{12EI}{l^3}c^2 & 0 & \frac{12EI}{l^3}cs & -\frac{12EI}{l^3}c^2 & 0 \\ & & 0 & 0 & 0 & 0 \\ & & & & -\frac{12EI}{l^3}cs & 0 \\ & & & & \frac{12EI}{l^3}c^2 & 0 \\ sym & & & & & 0 \end{bmatrix}. \tag{3}$$

In (2) and (3), $c = \cos\theta$ and $s = \sin\theta$; θ is the angle between the flexible boom and the global abscissa axis; a is the gravity acceleration; m is the total mass of the boom; and l is the total length of the boom. From (1), according to the vibration theory, the characteristic equation is

$$\left(K^{(0)} - \lambda_i^{(0)} M^{(0)}\right) A_i^{(0)} = 0. \tag{4}$$

In (4), for easy expression, set $\lambda_i^{(0)} = [\omega_i^{(0)}]^2$, which is the square of the i-order natural frequency of the flexible boom; $A_i^{(0)}$ is the vector of i-order mode shape. The flexible boom in crawler cranes or other large cranes has a relatively low luffing speed; the conclusion of the research in [22] shows that the natural frequency of the flexible boom is less affected by the large-scale motion when the boom is rotating at a relatively slower speed. Therefore, the first-order perturbation solution is used to solve the natural frequency of the flexible boom. For the mass matrix M and the stiffness matrix K of the flexible boom undergoing the large overall rotary motion, its first-order perturbation expansion formula is

$$\begin{cases} K = K^{(0)} + \eta K^{(1)}, \\ M = M^{(0)} + \eta M^{(1)}. \end{cases} \tag{5}$$

In (5), η, called the small perturbation parameter, is a positive number. When $\eta \longrightarrow 0^+$, the mass and stiffness matrices of large overall rotary motion were equal to their free vibration. On this basis, replacing the correlation matrix in (4), we can get the characteristic equation undergoing large overall rotary motion:

$$(K - \lambda_i M) A_i = 0. \tag{6}$$

Similarly, the natural frequency and the mode shape vector undergoing large overall rotary motion are first-order perturbation expanded, so the expansion polynomial is

$$\begin{cases} \lambda_i = \lambda_i^{(0)} + \eta\lambda_i^{(1)} + o(\eta^2), \\ A_i = A_i^{(0)} + \eta A_i^{(1)} + o(\eta^2). \end{cases} \tag{7}$$

Substituting (5) and (7) into (6), expanding it according to ascending powers of the small perturbation parameter, and omitting the infinitesimal, we can obtain the expression as follows:

$$\begin{aligned}&\left(K^{(0)}A_i^{(0)}-\lambda_i^{(0)}M^{(0)}A_i^{(0)}\right)+\eta\left(K^{(0)}A_i^{(1)}+K^{(1)}A_i^{(0)}-\lambda_i^{(0)}M^{(1)}A_i^{(0)}-\lambda_i^{(0)}M^{(0)}A_i^{(1)}-\lambda_i^{(1)}M^{(0)}A_i^{(0)}\right)\\&+\eta^2\left(K^{(1)}A_i^{(1)}-\lambda_i^{(1)}M^{(1)}A_i^{(0)}-\lambda_i^{(0)}M^{(1)}A_i^{(1)}-\lambda_i^{(1)}M^{(0)}A_i^{(1)}\right)=0.\end{aligned}\tag{8}$$

From the above formula, three equations about the first-order perturbation vibration and the free vibration parameters of the flexible boom can be obtained:

$$\begin{cases}K^{(0)}A_i^{(0)}=\lambda_i^{(0)}M^{(0)}A_i^{(0)},\\K^{(0)}A_i^{(1)}+K^{(1)}A_i^{(0)}=\lambda_i^{(0)}M^{(1)}A_i^{(0)}+\lambda_i^{(0)}M^{(0)}A_i^{(1)}+\lambda_i^{(1)}M^{(0)}A_i^{(0)},\\K^{(1)}A_i^{(1)}=\lambda_i^{(1)}M^{(1)}A_i^{(0)}+\lambda_i^{(0)}M^{(1)}A_i^{(1)}+\lambda_i^{(1)}M^{(0)}A_i^{(1)}.\end{cases}\tag{9}$$

According to the related theory of modal expansion method [23], the arbitrary mode shape of the first-order perturbation is written as the linear combination by each order of the free vibration mode shape vector:

$$A_i^{(1)}=a_{1i}A_1^{(0)}+a_{2i}A_2^{(0)}+\cdots+a_{ni}A_n^{(0)}=\sum_{k=1}^{n}a_{ki}A_k^{(0)},\tag{10}$$

where a_{ni} is the undetermined coefficient in the polynomial and subscripts k and i represent the modes order of the free vibration and first-order perturbation, respectively. Multiplying both sides of the second equation in (9) by the transpose matrix $[A_k^{(0)}]^{\mathrm{T}}$ of mode shape vector and substituting the combination form of (10) into it, we obtain (11) as follows:

$$\begin{aligned}\sum_{k=1}^{n}a_{ki}\left[A_k^{(0)}\right]^{\mathrm{T}}K^{(0)}A_k^{(0)}+\left[A_k^{(0)}\right]^{\mathrm{T}}K^{(1)}A_i^{(0)}&=\lambda_i^{(0)}\left[A_k^{(0)}\right]^{\mathrm{T}}M^{(1)}A_i^{(0)}+\\\lambda_i^{(0)}\sum_{k=1}^{n}a_{ki}\left[A_k^{(0)}\right]^{\mathrm{T}}M^{(0)}A_k^{(0)}&+\lambda_i^{(1)}\left[A_k^{(0)}\right]^{\mathrm{T}}M^{(0)}A_i^{(0)}.\end{aligned}\tag{11}$$

According to the mode shape orthogonality,

$$\text{when } i=k\begin{cases}\left[A_k^{(0)}\right]^{\mathrm{T}}M^{(0)}A_i^{(0)}=M_i^{(0)},\\\left[A_k^{(0)}\right]^{\mathrm{T}}K^{(0)}A_i^{(0)}=K_i^{(0)},\end{cases}\tag{12}$$

$$\text{when } i\neq k\begin{cases}\left[A_k^{(0)}\right]^{\mathrm{T}}M^{(0)}A_i^{(0)}=0,\\\left[A_k^{(0)}\right]^{\mathrm{T}}K^{(0)}A_i^{(0)}=0,\end{cases}\tag{13}$$

$$\lambda_i^{(0)}=\left[\omega_i^{(0)}\right]^2=\frac{\left[A_i^{(0)}\right]^{\mathrm{T}}K^{(0)}A_i^{(0)}}{\left[A_i^{(0)}\right]^{\mathrm{T}}M^{(0)}A_i^{(0)}}=\frac{K_i^{(0)}}{M_i^{(0)}}.\tag{14}$$

In the above formula, $M_i^{(0)}$ and $K_i^{(0)}$ are the main mass and the main stiffness of the i-order free vibration of the flexible boom. According to the conclusions in (12) and (13), when $i=k$, (11) can be expressed as

$$\begin{aligned}\sum_{k=1}^{n}a_{ki}\left(K_i^{(0)}-\lambda_i^{(0)}M_i^{(0)}\right)&=\lambda_i^{(0)}\left[A_i^{(0)}\right]^{\mathrm{T}}M^{(1)}A_i^{(0)}+\lambda_i^{(1)}M_i^{(0)}\\&-\left[A_i^{(0)}\right]^{\mathrm{T}}K^{(1)}A_i^{(0)}\Longleftrightarrow\lambda_i^{(1)}\\&=\frac{1}{M_i^{(0)}}\left[A_i^{(0)}\right]^{\mathrm{T}}K^{(1)}A_i^{(0)}\\&-\frac{\lambda_i^{(0)}}{M_i^{(0)}}\left[A_i^{(0)}\right]^{\mathrm{T}}M^{(1)}A_i^{(0)},\end{aligned}\tag{15}$$

and when $i\neq k$, (11) is expressed as

$$\begin{aligned}\sum_{k=1}^{n}a_{ki}\left(K_k^{(0)}-\lambda_i^{(0)}M_k^{(0)}\right)&=\lambda_i^{(0)}\left[A_k^{(0)}\right]^{\mathrm{T}}M^{(1)}A_i^{(0)}\\&-\left[A_k^{(0)}\right]^{\mathrm{T}}K^{(1)}A_i^{(0)}\Longleftrightarrow\sum_{k=1}^{n}a_{ki}\left(\lambda_k^{(0)}-\lambda_i^{(0)}\right)\\&=\frac{\lambda_i^{(0)}}{M_k^{(0)}}\left[A_k^{(0)}\right]^{\mathrm{T}}M^{(1)}A_i^{(0)}-\frac{1}{M_k^{(0)}}\left[A_k^{(0)}\right]^{\mathrm{T}}K^{(1)}A_i^{(0)}.\end{aligned}\tag{16}$$

Combining the above conclusion with (7), we obtain the expression as follows:

$$\begin{aligned}\lambda_i&=\lambda_i^{(0)}+\eta\left(\frac{1}{M_i^{(0)}}\left[A_i^{(0)}\right]^{\mathrm{T}}K^{(1)}A_i^{(0)}-\frac{\lambda_i^{(0)}}{M_i^{(0)}}\left[A_i^{(0)}\right]^{\mathrm{T}}M^{(1)}A_i^{(0)}\right)\\&+o\left(\eta^2\right).\end{aligned}\tag{17}$$

So far, an approximate solution to the first-order perturbation of the flexible boom undergoing large overall rotary motion is given. Through this method, the free-vibration natural frequency and mode shape vector can be used to approximately estimate the time-varying natural frequency of the flexible boom.

3.2. Natural Frequency Calculation of Flexible Boom. Through the perturbation theory, we specifically calculate the natural frequency of the flexible boom undergoing large overall rotary motion in this section. According to the perturbation expansion equation of mass matrix and stiffness matrix, we need to determine the small perturbation parameter and the specific expression of $M^{(1)}$ and $K^{(1)}$.

Adding the effect of angular velocity of the large overall rotary motion to the matrix listed in (2), take the element $M_{11,i}^{(0)}$ as an example:

$$\Delta M_{11,i}^{(0)} = \eta M_{11,i}^{(1)} = \frac{1}{t}\left[\frac{m_i}{3}\left(\cos^2\left(\theta_{0,i} + \varphi t\right) - \cos^2\theta_{0,i}\right) + \frac{13m_i}{35}\left(\sin^2\left(\theta_{0,i} + \varphi t\right) - \sin^2\theta_{0,i}\right)\right]. \tag{18}$$

In (18), set the small perturbation parameter $\eta = 1/t$, in which t is the time of the large overall rotary motion; $\theta_{0,i}$ is the initial angle of the boom; φ is angular velocity of the large overall rotary motion; and i is the boom unit number. Through the derivation of the above formula and adding it to all the elements in the free vibration mass matrix, the average perturbation matrix $M_i^{(1)}$ of the flexible boom during large overall rotary motion can be obtained, and the stiffness matrix can be obtained similarly.

Through the specific expression of the unit perturbation matrix, combining the dynamic equations, the perturbation matrix of the flexible boom can be formed.

This paper established flexible boom dynamic simulation models which can be divided into three units. The model has 21 generalized coordinates. Specific form as shown in Figure 3, counting up from the bottom, here is the unit 1 to unit 3 in order, where unit 1 is corresponding to the bottom joint of the boom, unit 2 is corresponding to the standard joint of the boom, and unit 3 is corresponding to the top joint of the boom. Each unit uses a separate floating frame to describe the flexible deformation, the origin of the floating coordinate system which is related to the unit 1 overlap with the origin of the global coordinate system.

The following are the specific values of the natural frequency of the 48 m flexible boom. Define the angular velocity of large overall rotary motion $\varphi = 1^\circ/s$. The first five-order modes of the boom-free vibration are listed in Table 1.

Through the mode shape vector in the above table, the first five-order natural frequency of the 48 m flexible boom under the large overall rotary motion can be calculated by (17), as shown in Table 2. From the table, it can be seen that the relation between first-order perturbation natural frequency and structure natural frequency is small when the angular velocity of the large overall rotary motion is low and thus cannot cause a large change in the natural frequency of the large overall rotary motion. The first-order perturbation natural frequencies are basically the same as the free vibration natural frequency. As the rotating angular velocity increases, according to (17), the first-order perturbation natural frequency increases linearly and the natural frequency of the large overall rotary motion also increases, and the calculation error of the first-order perturbation is gradually increasing; therefore, second-order or higher-order perturbation calculation should be used when the angular velocity is large.

4. Derivation of Similarity Relations of Flexible Truss Boom

4.1. Derivation of Complete Geometric Similarity Relations. In terms of the flexible truss boom that satisfied the Lagrange dynamical equation, its physical quantities involved include the gravitational acceleration a, the generalized force F, the boom movement time t, the boom length l, the material density ρ, elastic modulus of the boom material E, structural stress σ, and the boom natural frequency ω_n. The basic dimensions of each physical quantity are listed in Table 3.

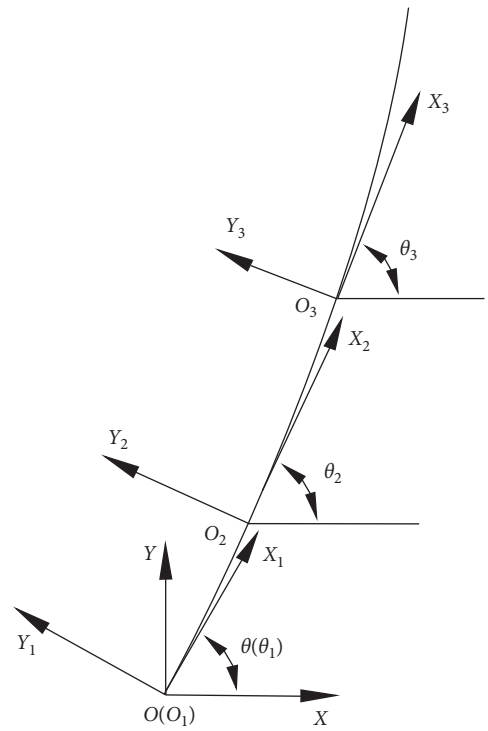

Figure 3: Division of flexible boom dynamic mode.

According to the principle of dimensional homogeneity, the following expressions are obtained:

$$\left(\mathrm{LT}^{-2}\right)^{n_1}\left(\mathrm{MLT}^{-2}\right)^{n_2}(\mathrm{T})^{n_3}(\mathrm{L})^{n_4}\left(\mathrm{ML}^{-3}\right)^{n_5}\left(\mathrm{ML}^{-1}\mathrm{T}^{-2}\right)^{n_6}\left(\mathrm{ML}^{-1}\mathrm{T}^{-2}\right)^{n_7}\left(\mathrm{T}^{-1}\right)^{n_8} = 1. \tag{19}$$

The equation about the index of each basic dimension is as follows:

$$\begin{cases} n_1 + n_2 + 0 + n_4 - 3n_5 - n_6 - n_7 + 0 = 0, \\ 0 + n_2 + 0 + 0 + n_5 + n_6 + n_7 + 0 = 0, \\ -2n_1 - 2n_2 + n_3 + 0 - 3n_5 - 2n_6 - 2n_7 - n_8 = 0. \end{cases} \tag{20}$$

It can be concluded that the rank of the coefficient matrix of the above equations system is equal to 3, so five independent similarity criteria are needed to derivate the similarity relation of the truss boom.

Assuming that the values of the independent index in the above equations system are 1, and according to the same index, five similarity criteria for the truss boom can be obtained after recombining as follows:

Table 1: Mode shape vector of 48 m flexible boom.

		First-order mode A1 (mm)	Second-order mode A2 (mm)	Third-order mode A3 (mm)	Fourth-order mode A4 (mm)	Fifth-order mode A5 (mm)
Top node of bottom joint	Axis X_1 direction	7.73×10^{-17}	2.01×10^{-3}	-4.84×10^{-17}	2.32×10^{-17}	1.51×10^{-16}
	Axis Y_1 direction	5.81×10^{-3}	-1.81×10^{-16}	4.38×10^{-17}	-7.53×10^{-3}	-9.09×10^{-3}
	Axis Z_1 direction	9.67×10^{-7}	-7.19×10^{-7}	1.06×10^{-20}	-5.75×10^{-6}	3.18×10^{-6}
Top node of standard joint	Axis X_2 direction	-1.03×10^{-16}	9.52×10^{-3}	2.56×10^{-17}	-2.39×10^{-17}	-6.39×10^{-17}
	Axis Y_2 direction	-8.51×10^{-3}	4.15×10^{-17}	-1.38×10^{-16}	-2.33×10^{-4}	-8.47×10^{-3}
	Axis Z_2 direction	5.67×10^{-7}	9.35×10^{-7}	1.19×10^{-20}	-4.51×10^{-6}	-9.35×10^{-7}
Top node of top joint	Axis X_3 direction	-4.30×10^{-17}	1.03×10^{-2}	2.49×10^{-20}	6.55×10^{-17}	-2.10×10^{-16}
	Axis Y_3 direction	-3.75×10^{-3}	2.14×10^{-16}	4.75×10^{-17}	7.61×10^{-3}	1.40×10^{-3}
	Axis Z_3 direction	8.25×10^{-6}	3.18×10^{-6}	5.33×10^{-20}	5.98×10^{-6}	7.56×10^{-6}

$$\begin{aligned}
\pi_1 &= \frac{at^2}{l}, \\
\pi_2 &= \frac{F}{tl^4\rho}, \\
\pi_3 &= \frac{E}{tl^2\rho}, \\
\pi_4 &= \frac{\sigma}{tl^2\rho}, \\
\pi_5 &= t\omega_n.
\end{aligned} \tag{21}$$

The similarity ratio between physical quantities is defined as

$$\begin{aligned}
\frac{t^m}{t^p} &= S_t, \\
\frac{\omega_n^m}{\omega_n^p} &= S_\omega, \\
\frac{\sigma^m}{\sigma^p} &= S_\sigma, \\
\frac{E^m}{E^p} &= S_E, \\
\frac{l^m}{l^p} &= S_l, \\
\frac{\rho^m}{\rho^p} &= S_\rho, \\
\frac{F^m}{F^p} &= S_F.
\end{aligned} \tag{22}$$

Table 2: Natural frequency of 48 m flexible boom undergoing large overall motion.

Modal order	Free vibration natural frequency (Hz)	First-order perturbation natural frequency (Hz)	Large overall rotary motion of natural frequencies (Hz)
1	0.7039	0.019	0.7042
2	1.3082	0.045	1.3090
3	7.5759	0.055	7.5761
4	9.0312	0.157	9.0326
5	20.7294	0.260	20.7310

Table 3: Fundamental dimensions of the flexible boom.ρ

Physical quantity	Basic dimension composition
Gravity acceleration, a	LT-2
Generalized force, F	MLT-2
Boom movement time, t	T
Boom length, l	L
Material density, ρ	ML-3
Material elastic modulus, E	ML-1T-2
Structural stress, σ	ML-1T-2
Boom natural frequency, ω_n	T-1

For the prototype and the model, through the similarity criterion in (21), respectively, the similarity relations can be obtained as follows:

$$\begin{cases}
S_\omega = \dfrac{1}{S_t} = \sqrt{\dfrac{S_E}{S_l^2} \cdot S_\rho}, \\
S_E = S_\sigma, \\
S_F = S_l^2 \cdot S_E.
\end{cases} \tag{23}$$

Equation (23) is the complete similarity relation of the truss boom geometry.

4.2. Derivation of Dynamic Characteristics Similarity Relations. Based on the complete flexible boom dynamic equation, the similarity relation between the dynamic parameters can be accurately derived by the equational analysis method. By means of introducing the similarity ratio between each physical quantity and the natural frequency of the flexible boom, the similarity relations between the dynamic parameters are solved; the specific similarity ratio between dynamic parameters of the boom with given parameters is obtained.

In allusion to the flexible boom dynamic equation, there are five similarity relation types of the single-valued parameters between the similar model and the prototype: (1) similar geometrical conditions; (2) similar mass; (3) similar load excitation; (4) similar physical conditions; (5) similar in time, that natural frequency is similar.

In order to accord with actual situation, the flexible boom prototype and model use the same material; that is, $S_\rho = S_E = 1$. In addition to the above five similarity relation types, it is also necessary to ensure that the boundary conditions and initial conditions of the prototype and the model should be the same, to eliminate the impact on the similarity relation of the boom. Relative to the length of the boom, the flexible deformation is numerically negligible; therefore, in the similarity ratio matrix, the coupling term ignores the effect of generalized deforming coordinates.

First of all, the similarity ratio of generalized coordinates is

$$S = \left[S_{ix}, S_{iy}, S_{\theta,i}, S_{1,i}, S_{2,i}, S_{3,i}, S_{4,i}, S_{5,i}, S_{6,i}\right]^{\mathrm{T}}. \tag{24}$$

The similarity ratio matrix of the mass matrix is

$$S^M = \frac{\left(M_i^m\right)_{9\times 9}}{\left(M_i^p\right)_{9\times 9}} = \begin{bmatrix} S_aS_l & 0 & S_aS_l^2 & S_aS_l & S_aS_l & S_aS_l^2 & S_aS_l & S_aS_l & S_aS_l^2 \\ & S_aS_l & S_aS_l^2 & S_aS_l & S_aS_l & S_aS_l^2 & S_aS_l & S_aS_l & S_aS_l^2 \\ & & S_aS_l^3 & S_aS_l & S_aS_l^2 & S_aS_l^3 & S_aS_l & S_aS_l^2 & S_aS_l^3 \\ & & & S_aS_l & 0 & 0 & S_aS_l & 0 & 0 \\ & & & & S_aS_l & S_aS_l^2 & 0 & S_aS_l & S_aS_l^2 \\ & & & & & S_aS_l^3 & 0 & S_aS_l^2 & S_aS_l^3 \\ & & & & & & S_aS_l & 0 & 0 \\ & & & & & & & S_aS_l & S_aS_l^2 \\ sym & & & & & & & & S_aS_l^3 \end{bmatrix}. \tag{25}$$

The similarity ratio matrix of the stiffness matrix is

$$S^K = \frac{\left(K_i^m\right)_{9\times 9}}{\left(K_i^p\right)_{9\times 9}} = \begin{bmatrix} 0_{3\times 3} & & & 0_{3\times 6} & & \\ & \frac{S_a}{S_l} & 0 & 0 & \frac{S_a}{S_l} & 0 & 0 \\ & & \frac{S_H^2S_a}{S_l^3} & \frac{S_H^2S_a}{S_l^2} & 0 & \frac{S_H^2S_a}{S_l^3} & \frac{S_H^2S_a}{S_l^2} \\ 0_{6\times 3} & & & \frac{S_H^2S_a}{S_l} & 0 & \frac{S_H^2S_a}{S_l^2} & \frac{S_H^2S_a}{S_l} \\ & & & & \frac{S_a}{S_l} & 0 & 0 \\ & & & & & \frac{S_H^2S_a}{S_l^3} & \frac{S_H^2S_a}{S_l^2} \\ sym & & & & & & \frac{S_H^2S_a}{S_l} \end{bmatrix}. \tag{26}$$

In the same way, according to the generalized force calculation method of the flexible boom unit in the luffing plane, substituting the similarity ratio between loads, the similarity ratio of the generalized force of each unit can be obtained:

$$F_{S,i} = \sum_{n=1}^{k} F_{n,i},$$

$$S^F = \frac{\left(F_{S,i}^m\right)_{9\times 1}}{\left(F_{S,i}^p\right)_{9\times 9}} = \left[S_{1,i}^F, S_{2,i}^F, S_{3,i}^F, S_{4,i}^F, S_{5,i}^F, S_{6,i}^F, S_{7,i}^F, S_{8,i}^F, S_{9,i}^F\right]^{\mathrm{T}}. \tag{27}$$

Through the equational analysis method, the similarity relation between the dynamic parameters of the top joint of the boom is derived, according to the specific expression of the dynamic equation of the flexible boom as follows:

$$\begin{aligned} &M_{17,3}\cdot\ddot{r}_{3x} + M_{27,3}\cdot\ddot{r}_{3y} + M_{37,3}\cdot\ddot{\theta}_3 + M_{47,3}\cdot\ddot{u}_{1,3} \\ &\quad + M_{77,3}\cdot\ddot{u}_{4,3} + K_{47,3}\cdot u_{1,3} + K_{77,3}\cdot u_{4,3} \\ &\quad + \dot{\theta}_1^2\left(M_{47,3}\cdot u_{1,3} + M_{77,3}\cdot u_{4,3}\right) \\ &\quad + 2\dot{\theta}_1\left(\widetilde{M}_{57,3}\cdot\dot{u}_{2,3} + \widetilde{M}_{67,3}\cdot\dot{u}_{3,3}\right. \\ &\quad \left. + \widetilde{M}_{78,3}\cdot\dot{u}_{5,3} + \widetilde{M}_{79,3}\cdot\dot{u}_{6,3}\right) = F_{S7,3}. \end{aligned} \tag{28}$$

Substituting the physical quantities of the prototype and the model into the above formula, it is easy to get the relations between the similarity ratios:

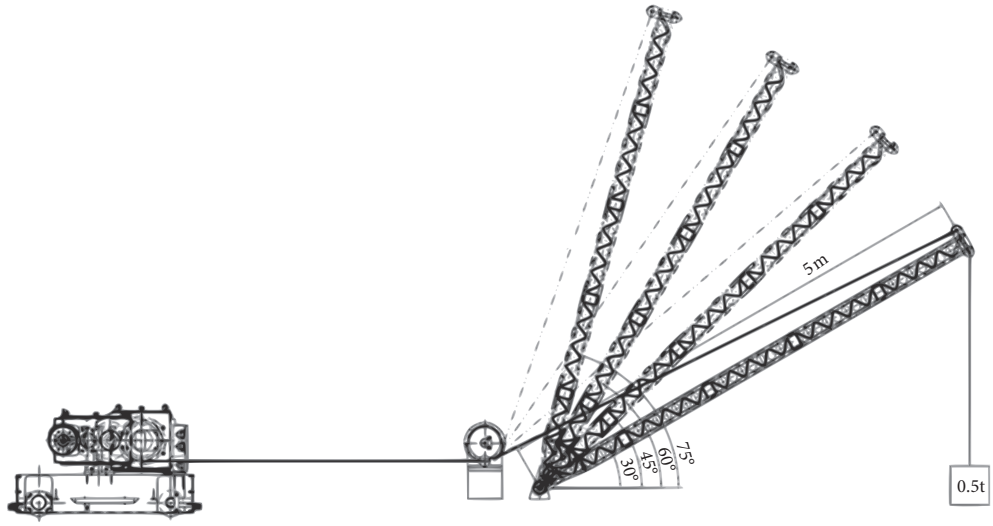

Figure 4: Experimental conditions.

Table 4: The design parameters of model experiments.

The boom number	The boom length	The boom section parameters	The angle of luffing
1	3 m	150 × 160	30°~70°
2	4 m	150 × 160	
3	5 m	150 × 160	
4	3 m	300 × 320	
5	4 m	300 × 320	
6	5 m	300 × 320	

$$\begin{cases} S^{M}_{17,3}\cdot\dfrac{S_{3x}}{S_t^2}=S^{M}_{27,3}\cdot\dfrac{S_{3y}}{S_t^2}=S^{M}_{37,3}\cdot\dfrac{S_{\theta,3}}{S_t^2}=S^{M}_{47,3}\cdot\dfrac{S_{1,3}}{S_t^2}=S^{M}_{77,3}\cdot\dfrac{S_{4,3}}{S_t^2}=S^{F}_{7,3}, \\ S^{K}_{47,3}\cdot S_{1,3}=S^{K}_{77,3}\cdot S_{4,3}=S^{M}_{47,3}\cdot\dfrac{S_{1,3}}{S_t^2}, \\ \left(\dfrac{S_{\theta,1}}{S_t}\right)^2\cdot S^{M}_{47,3}\cdot S_{1,3}=\left(\dfrac{S_{\theta,1}}{S_t}\right)^2\cdot S^{M}_{77,3}\cdot S_{4,3}=S^{F}_{7,3}, \\ \dfrac{S_{\theta,1}}{S_t}\cdot\widetilde{S}^{M}_{57,3}\cdot\dfrac{S_{2,3}}{S_t}=\dfrac{S_{\theta,1}}{S_t}\cdot\widetilde{S}^{M}_{67,3}\cdot\dfrac{S_{3,3}}{S_t}=\dfrac{S_{\theta,1}}{S_t}\cdot\widetilde{S}^{M}_{78,3}\cdot\dfrac{S_{5,3}}{S_t}=\dfrac{S_{\theta,1}}{S_t}\cdot\widetilde{S}^{M}_{79,3}\cdot\dfrac{S_{6,3}}{S_t}=S^{F}_{7,3}. \end{cases} \tag{29}$$

Through the similarity ratios between the mass matrix, the stiffness matrix, and the generalized force, the similarity relations between the dynamic parameters and the physical quantities of the flexible boom can be obtained by the above formula. Using the above derivation method, based on the other equations in the equation system, the similarity relations between the other dynamic parameters of the boom can be obtained, and the derivation progress will not be repeated here.

5. Similarity Model Experiment and Result Analysis of Crane Flexible Truss Boom

In allusion to the research object of this article, a scale-down boom model for similarity model experiment is designed. The larger slenderness ratio is the most obvious feature of the flexible boom. Therefore, the experimental model of the boom was constructed in the form of a truss type and had larger slenderness ratio. The experimental boom model was divided into two sections; each section had three kinds of boom length, in order to verify the correctness of the similarity relations from two aspects of the cross-sectional size and boom length of the flexible boom. The acquisition of experimental data was achieved by several groups of displacement sensors; these sensors were fixed in several key positions on the boom model, and all kinds of dynamic data were transmitted in real time during the experiment. Experimental conditions are as shown in Figure 4.

In order to verify the dynamic similarity relations, 6 groups of parameters of the boom are designed and listed in Table 4, to verify the correctness of the similarity relations through experimental data analysis.

(a) (b)

Figure 5: The structure of model boom: (a) experiment model 1; (b) experiment model 2.

Table 5: The sensor types of model experiments.

The measuring point number	Position	Sensor type
1	Junction of standard joint and bottom joint	Acceleration sensor
2	Junction of standard joint and top joint	Acceleration sensor
3	The vertex of top joint	Acceleration sensor
4	Hinged point of the boom root	Gyroscope angular velocity sensor

Table 6: The arrangement of the experiments.

Comparative results	The number of prototype booms	The number of model booms	Dynamic parameters
First group	2	3	The lateral deformation of point 3
Second group	5	6	The lateral deformation of point 3
Third group	1	6	The lateral deformation of point 3
Fourth group	1	3	The longitudinal deformation of point 2

Table 7: Similarity ratio and average error of group 1.

Project	Value
Similarity ratio of generalized force, $S_{7,3}^F$	1.051
Average similarity ratio of natural frequency, S_ω	0.654
Similarity ratio of the lateral deformation of point 3, $u_{5,3}$	1.966
Relative error of the maximum deformation by similarity prediction	13.7%

Table 8: Similarity ratio and average error of group 2.

Project	Value
Similarity ratio of generalized force, $S_{7,3}^F$	1.089
Average similarity ratio of natural frequency, S_ω	0.669
Similarity ratio of the lateral deformation of point 3, $u_{5,3}$	1.947
Relative error of the maximum deformation by similarity prediction	19.1%

Table 9: Similarity ratio and average error of group 3.

Project	Value
Similarity ratio of generalized force, $S_{7,3}^F$	0.876
Average similarity ratio of natural frequency, S_ω	0.696
Similarity ratio of the lateral deformation of point 3, $u_{5,3}$	1.083
Relative error of the maximum deformation by similarity prediction	14.1%

The truss boom structure used in the experiment is assembled from three parts: bottom joint, standard joint, and top joint plate. The objects are shown in Figure 5.

In order to obtain the dynamic parameters of multiple positions of the boom, three measuring points are designed to collect the deformation and deformation frequency information of the boom; sensor types which are installed at each measuring point are listed in Table 5.

Table 10: Similarity ratio and average error of group 4.

Project	Value
Similarity ratio of generalized force, $S_{7,3}^F$	1.135
Average similarity ratio of natural frequency, S_ω	0.377
Similarity ratio of the longitudinal deformation of point 2, $u_{1,3}$	4.782
Relative error of the maximum deformation by similarity prediction	28.7%

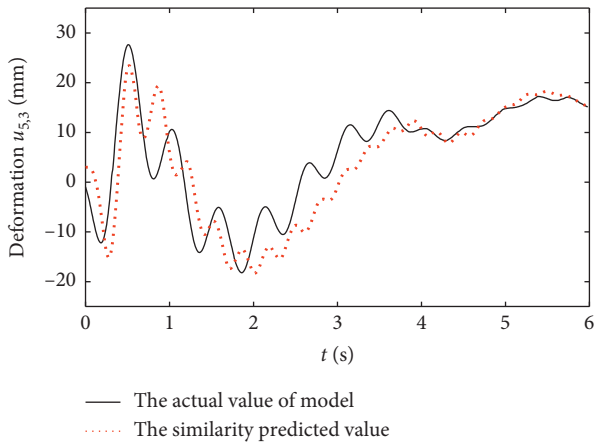

Figure 6: The lateral deformation comparison of point 3 in group 1.

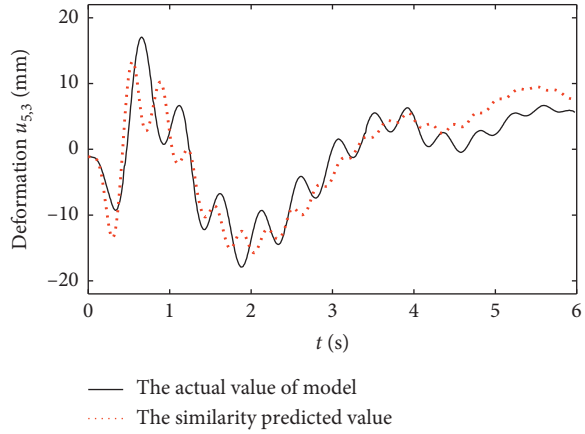

Figure 7: The lateral deformation comparison of point 3 in group 2.

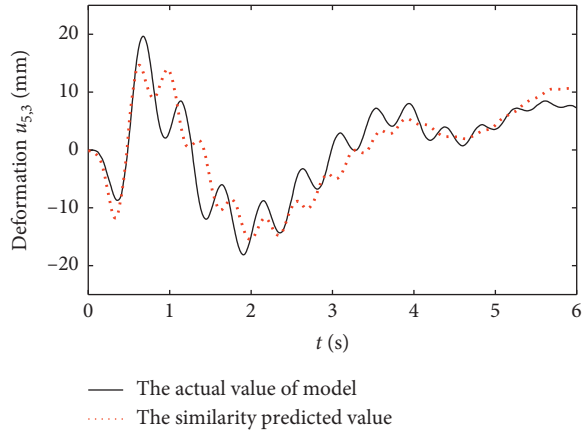

Figure 8: The lateral deformation comparison of point 3 in group 3.

According to the experimental result data, based on the arrangement of the prototype and the model listed in Table 6, by using the similarity relation of dynamic characteristics of the flexible boom, the actual value of the boom model and the similarity predicted value are compared.

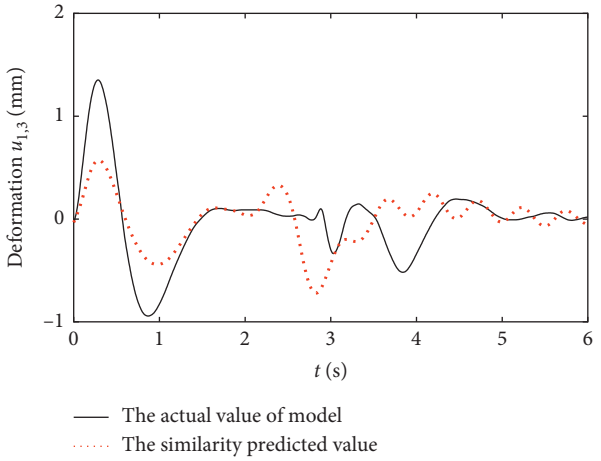

Figure 9: The longitudinal deformation comparison of point 2 in group 4.

Tables 7–10 show the similarity ratio of various dynamic parameters in the comparison of experimental results from group 1 to group 4 and give the average error between the actual value of the model and the predicted value of the similarity relation.

From Figures 6–9, it can be seen that, in the initial stage of the experiment, due to the impact of the load shock, the measuring point 3 of top joint of the boom has obvious deformation, then it enters the uniform luffing stage, and the lateral deformation of the measuring point slowly increases. When calculating the error of maximum deformation, predicted by the similarity relations, deformation caused by load shock in the initial stage is excluded, the curve trend of the model is consistent with that of the prototype, and large deformation errors caused by load shock in the initial stage are excluded. The average absolute error of deformation prediction results by using theoretical similarity relation was 15.6%, and the other similarity predicted values were basically accurate.

6. Conclusions

This paper derived the similarity relations of natural frequency and other physical quantities of the crane truss boom by using the dimension analysis method of similarity theory when geometric parameters are completely similar; in order to obtain the approximate natural frequency of the boom with flexible deformation undergoing the large overall rotary motion, combining the perturbation theory with modal analysis, an approximate calculation method of natural frequency of crane boom with flexible deformation was proposed in this paper. Then, the boom parameters of the crawler crane which working on the luffing plane were calculated. The results show that because the luffing frequency of the crawler crane boom is much lower than its structural natural frequency, the large overall rotary motion has little effect on its natural frequency. Finally, the similarity relations of dynamic parameters of the boom were derived by the equational analysis method.

A similarity model experiment was designed to verify the similarity relations of the dynamic characteristics of the flexible truss booms. Based on the typical luffing conditions, the dynamic parameters of the scale-down boom model are obtained by the corresponding sensors installed on the boom. Comparing the related parameters of prototype and similar model of experiment, the correctness of the dynamic similarity of crane flexible truss boom was verified. It proved that, by using the similarity relations of the flexible boom derived in this paper, the model parameters can be well predicted through the prototype dynamic parameters.

Data Availability

The data used to support the findings of this study are available from the corresponding author upon request.

Conflicts of Interest

The authors declare that they have no conflicts of interest.

Acknowledgments

This work was supported by the National Natural Science Foundation of China (Grant no. 51475068).

References

[1] G. Wang, C. H. Qi, and X. C. Kong, "Geometric nonlinear analysis for crane main and sub-boom structures with mechanism displacements," *Engineering Mechanics*, vol. 32, no. 7, pp. 210–218, 2015.

[2] Y. Huang, G. Guo, M. Y. Tang, and W. Hu, "Active control of slewing vibration in an ultra-long flexible boom," *Journal of Vibration and Shock*, vol. 35, no. 6, pp. 137–140, 2016.

[3] B. H. Wang and P. M. Lu, "Vibration mechanism of arm system of concrete pump truck," *Journal of Vibration and Shock*, vol. 30, no. 9, pp. 259–263, 2011.

[4] T. J. Mueller and J. M. Robertson, "A study of the mean motion and turbulence downstream of a roughness element," *Development in Theoretical and Applied Mechanics*, vol. 1, pp. 326–340, 1963.

[5] W. De Silva, *Dynamic Testing and Seismic Qualification Practice*, Lexington Books, Lanham, MD, USA, 1983.

[6] D. Vassalos, "Physical modelling and similitude of marine structures," *Ocean Engineering*, vol. 26, no. 2, pp. 111–123, 1998.

[7] J. Chen, M. Wang, and S. Fan, "Experimental investigation of small-scaled model for powerhouse dam section on shaking table," *Structural Control and Health Monitoring*, vol. 20, no. 5, pp. 740–752, 2013.

[8] Z. Luo, Y. P. Zhu, Q. K. Han, D. Y. Wang, and Y. Q. Liu, "Review and prospect for dynamic similitude theory and its applications in the structure vibration," *Journal of Mechanical Engineering*, vol. 52, no. 23, pp. 114–134, 2016.

[9] J. D. Singleton and J. W. T. Yeager, "Important scaling parameters for testing model-scale helicopter rotors," *Journal of Aircraft*, vol. 37, no. 3, pp. 396–402, 1998.

[10] X. Q. Luo, S. G. Cheng, Z. H. Zhang et al., "Study of similarity theory of geomechanical model test in electromagnetic field," *Yantu Lixue/Rock and Soil Mechanics*, vol. 32, no. 4, pp. 1035–1039, 2011.

[11] J. S. Nam, Y. J. Park, J. K. Kim, J. W. Han, Y. Y. Nam, and G. H. Lee, "Application of similarity theory to load capacity of gearboxes," *Journal of Mechanical Science and Technology*, vol. 28, no. 8, pp. 3033–3040, 2014.

[12] A. Jha and R. Sedaghati, "Dynamic testing of structures using scale models," in *Proceedings of the 46th AIAA/ASME/ASCE/AHS/ASC Structures, Structural Dynamics and Materials Conference*, Austin, TX, USA, April 2005.

[13] S. D. Wang, D. S. Yang, S. G. Shi, and R. Y. Zhang, "Prediction of vibration response and sound radiation of the underwater complex shell by using similitude principle," *Journal of Vibration and Shock*, vol. 24, no. 3, pp. 4–8, 2005.

[14] S.-d. Wang, D.-s. Yang, and N. Liu, "Investigation of acoustic scale effects and boundary effects for the similitude model of underwater complex shell-structure," *Journal of Marine Science and Application*, vol. 6, no. 1, pp. 31–35, 2007.

[15] F. Liu, F. Z. Pang, D. F. Han, and X. H. Miu, "Moving boundary similarity method and its application in ship structural dynamics analysis," *Journal of Vibration and Shock*, vol. 33, no. 20, pp. 111–117, 2014.

[16] Q. H. Dai, P. Ji, C. B. Yin, D. S. Yi, B. Wang, and J. Zhu, "Application of similitude theory for welding deformation prediction of large hydraulic excavator," *Applied Mechanics and Materials*, vol. 26–28, pp. 448–451, 2010.

[17] Y. L. Jin and T. H. Wu, "Dynamic similarity analysis and experimental verification on a quayside bridge container crane," *Journal of Shanghai Jiaotong University*, vol. 46, no. 10, pp. 1609–1615, 2012.

[18] H. Chen and N. Sun, "Nonlinear control of underactuated systems subject to both actuated and unactuated state constraints with experimental verification," *IEEE Transactions on Industrial Electronics*, 2019.

[19] H. Chen, B. Xuan, P. Yang, and H. Chen, "A new overhead crane emergency braking method with theoretical analysis and experimental verification," *Nonlinear Dynamics*, vol. 98, no. 3, pp. 2211–2225, 2019.

[20] N. Sun, Y. Fu, T. Yang et al., "Nonlinear motion control of complicated dual rotary crane systems without velocity feedback: design, analysis and hardware experiments," *IEEE Transactions on Automation Science and Engineering*, 2019.

[21] M.-R. Xu, S.-P. Xu, and H.-Y. Guo, "Determination of natural frequencies of fluid-conveying pipes using homotopy perturbation method," *Computers & Mathematics with Applications*, vol. 60, no. 3, pp. 520–527, 2010.

[22] Y.-R. Wang and Z.-W. Fang, "Vibrations in an elastic beam with nonlinear supports at both ends," *Journal of Applied Mechanics and Technical Physics*, vol. 56, no. 2, pp. 337–346, 2015.

[23] L. Lin, X. Zhang, Y. Li, and G. G. Cheng, "Transmission loss analysis of two-dimensional mufflers based on modal expansion method," *Journal of Vibration and Shock*, vol. 30, no. 11, pp. 161–164+174, 2011.